AMANDA-IR/20011101 2001 November 15

Preliminary Results from AMANDA-II/2000 Data

Sebastian Böser, Tonio Hauschildt, Marek Kowalski, Mathieu Ribordy,
C .Spiering, Peter Steffen, Ralf Wischnewski
DESY Zeuthen

November 14th, 2001

Abstract

We describe the May 2001 status of the analysis effort at DESY-Zeuthen on the first data taken with the completed AMANDA-II detector in 2000. A preliminary analysis of a small data set indicates, that the detector performs properly. We estimate, that the separation of atmospheric ν_μ's from the background of atmospheric μ's will be possible with a higher efficiency and better angular coverage, as compared to the AMANDA-B10 analysis. This report was made available to the DESY-PRC on May 17/18, 2001. [1]

1 Introduction

In the austral summer season of 1999/2000, the AMANDA-II detector was completed to its final form, consisting of 680 optical modules and 19 strings. The subject of this report is the first analysis of the data, taken with the full AMANDA-II detector in 2000. Since this analysis is heavily based on the knowledge gathered during the analysis of the subdetectors AMANDA-B4 and B-10, we briefly summarize the previous efforts. The history of the AMANDA deployment is shown in table 1.1. Even though the analysis of the data taken with the AMANDA-B4 detector produced important methodical results [1], it was the data taken with the AMANDA-B10 detector which has lead to large improvement

[1] We feel that this note, originally written for the members of the DESY-PRC, is also a valuable AMANDA-Internal Report, since some basic A-II ν-cuts turn out to be stable since spring and the detailed consistency checks done with 1997/B10 data are relevant for ongoing 98/99 ananlysis. This internal report is a slightly extended version of the original PRC report (Figures 4.5 and 4.6 are added to give a consistent picture of the A-II trigger acceptance). We note, that the final ν-passing rate as quoted in Sect.7 is the "very-preliminary" number as obtained by that time; in the current analyses it is reduced by eliminating some of the remaining background, which was already mentioned there.

of our detector understanding and to the physics results presented recently [2]. E.g. it became clear that depth dependent ice properties had to be incorporated into a realistic detector simulation. This and other improvements resulted in several repetitions of the analysis of the 97-data. The search for ν_μ neutrinos has finally lead to the separation of about 260 atmospheric ν_μ candidates [2, 3, 4].

1995/1996	deployment of first 4 strings (86 OMs) AMANDA-B4: 4 strings, 86 OMs
1996/1997	deployment of 6 strings strings (216 OMs) AMANDA-B10: 10 strings, 302 OMs
1997/1998	deployment of 3 strings strings (126 OMs) AMANDA-B13: 13 strings, 428 OMs
1999/2000	deployment of 5 strings strings (252 OMs) AMANDA-II: 19 strings, 680 OMs

Table 1.1: History of AMANDA deployment

The analysis of the 1998, 1999, and 2000 data was started in a parallel effort at the beginning of 2001 at different laboratories. DESY-Zeuthen is focussing on the analysis of the 2000 data. The current status will be reported here.
In November 2000, after the first year of operation of the complete AMANDA-II detector, two tape copies of the data were send to LBNL and DESY-Zeuthen.
The analysis of the data is still an iterative process. It consists of several steps:

- Analysis of detector performance to select useful run periods and optical modules. Validation of new technology components.
- Determination of the calibration constants.
- Simulation of signal events from atmospheric neutrinos and background events from cosmic muons.
- Comparison of AMANDA-B10 data from 1997 with data restricted to the same strings in 2000.
- Neutrino Filter Level 1&2: Data reduction to $\sim$7%(level-1) and $\sim$0.3%(level-2) for a subsample of the 2000 data.
- Final Filtering: First steps towards the selection of ν_μ candidates.

With improved understanding, some of these steps will be repeated until the complete data are analyzed and the final atmospheric ν-sample is obtained. The final sample will be used for further and more detailed analysis, like a search for point sources and diffuse high energy neutrinos.
At present we are close to the end of the first path. In the following we are going to describe the details of the different steps.

2 Data sample and detector performance

Since completion in February 2000, AMANDA-II runs with a Majority Trigger of 24 within a time window of 2.5μs (i.e. $\geq$24 OMs fired). The rate due to this muon trigger is 60-70 Hz, additional triggers (String, SPASE, AMANDA-A, A&B) added with a few Hz each, yielding a total of about 5 GB raw data per day. The data collected between February, 15th and November, 6th amount to $\sim$1.2 TB in 608 runs in 265 calendar days. The corresponding 92 DLT-Tapes are currently uploaded to the TapeRobot at DESY-Zeuthen. Table 2 gives an overview on the experimental settings, typical total raw trigger rates, data volumes and livetimes since 1997 [1].

	Muon Trigger	Total Triggerrate	Livetime	Data Volume	Location
1997	$\geq$16	75 Hz	130 d	0.56 TB	LBNL,DESY
1998	$\geq$12	110 Hz	?	1.5 TB	LBNL,DESY
1999	$\geq$18	60 Hz	?	0.9 TB	LBNL
2000	$\geq$24	70 Hz	[$\leq$195 d]	1.2 TB	(LBNL,DESY)

Table 2.2: AMANDA Muon trigger settings, total trigger rates, effective livetime and data availability.

Apart from being larger in number of PMTs compared to the B-10 detector, AMANDA-II contains several new detector components: Analog-Fiber-OM technology, dAOMs (with LEDs and LaserDiodes) and the first prototype DOM-string (with parallel AOM-LED readout). All types of these new modules, including their front-end boards (SWAMP/ORB-amplifiers), as well as the newly installed majority trigger system (DMADD) need to be tracked in their performance (X-talk, stability, sensitivity drop on strings 11-13). The 2000 analysis is the first experimental verification of the Analog-Fiber-OM technology by muon track reconstruction (Fiber-OMs were first deployed in 1997, and with strings 11-13 in 1998).
The detailed daily performance of the detector was studied so far only for the 1997 data sample (see [4, 5, 6, 7]). Standard algorithms and tools are still under development. For a first scan of the main detector characteristics over the year 2000, we extracted statistics information from a sample of raw data files spread over the whole run period (satellite data collected over the year, and first data uploadad from DLTs). A `Root`-ntuple allows to scan for bad run periods, and also to check stability of individual PMTs for each run. We selected a set of good quality runs (around day 140) for the analysis presented here, a list of bad PMTs is used for a preliminary cleaning the experimental data (see section 5 and 6).
The nominal uptime of the detector was high ($\geq$90%). However, failure of hardware components over the year, partially undetected due to the absence of routine monitoring of the AMANDA detector, lead to a reduction of livetime [2]. It can be estimated after the

[1] Livetime for 2000 is an upper limit, estimated from nominal uptime and DAQ-efficiency.
[2] Such a monitoring system has been put in place in 2001.

full data set has been scanned.
A total of 343 data files has been used for a first quality assessment. Figure 2.1 shows the number of "suspect" data channels (dead, high-rate and unstable PMTs and/or surface electronics[3]) as a function of the day in 2000. Periods of different quality can be already seen with this limited data set (1.4% of all data).

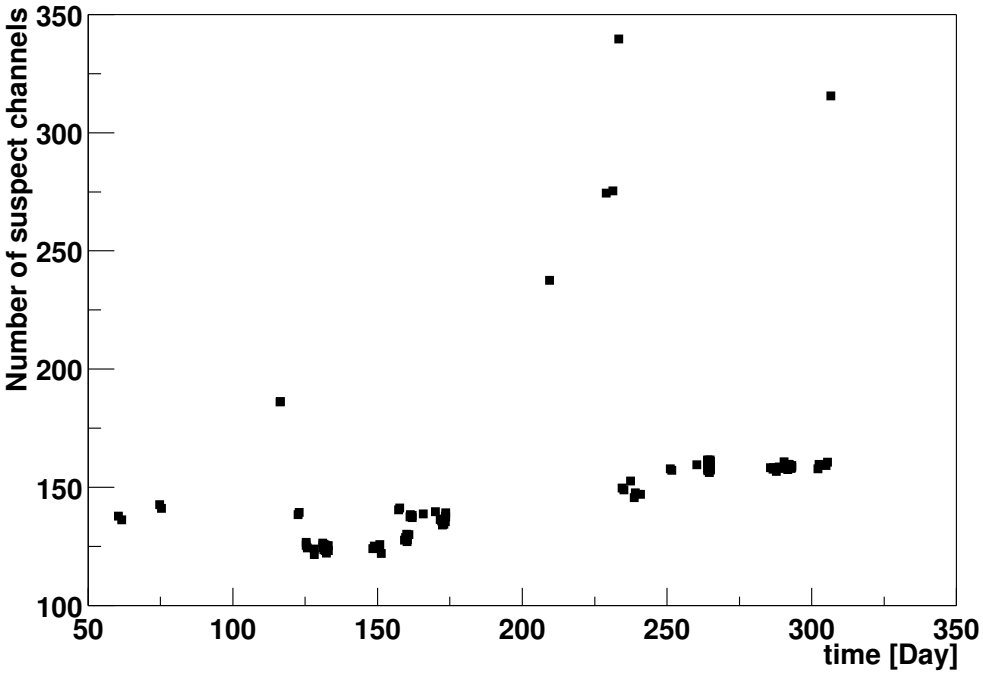

Figure 2.1: Number of "suspect" data channels as a function of the day in 2000 for a small selection of files.

In figure 2.2 the raw trigger rate of the muon trigger is displayed as a function of the day in 2000. This rate, being dominated by downgoing atmospheric muons generated in the upper atmosphere, shows the expected seasonal behaviour with a maximum towards austral summer and a minimum around day 200-250, as observed before for 1997 AMANDA data in [6]. Also the absolute size of this effect (a 5-7% rate drop between day 100 and 250) is reproduced, even though at this stage no cleaning of unstable PMTs or dead-time correction has been done. We are thus confident that extended quality analysis will result in a subset of stable OMs.
We emphasize, that despite the encouraging results presented in the next sections, several low-level checks of the detector remain to be done. They will yield a better quantitative description of such basic variables as absolute trigger rates, elementary response of detector channels and high multiplicity events. Transient effects due to unstable OMs and

[3]This number includes PMTs dead since deployment.

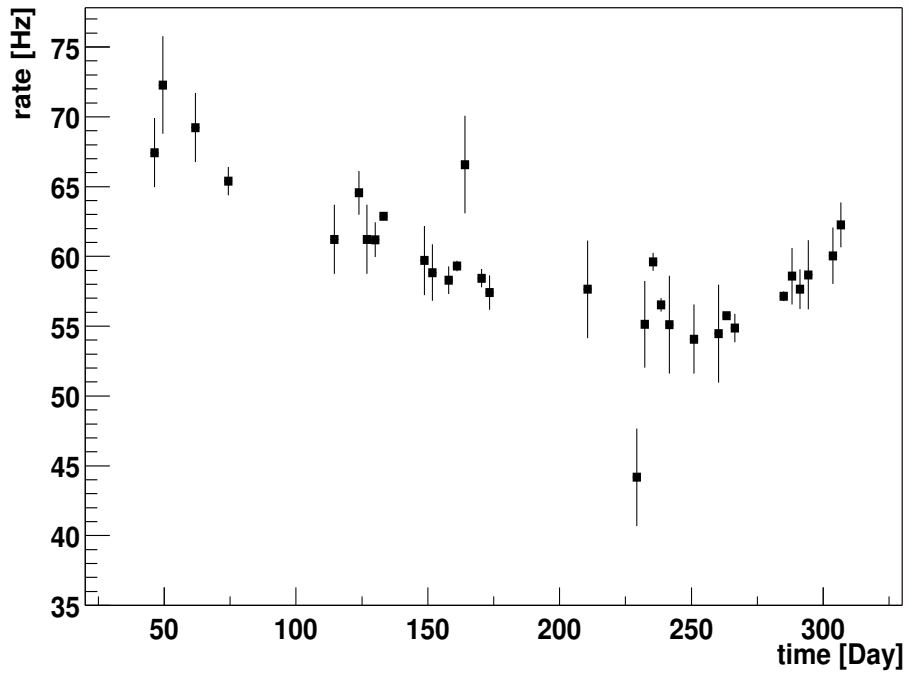

Figure 2.2: Raw muon trigger rate as function of day in 2000 for a small subset of files, with a rate variation as expected from seasonal muon flux variation.

surface components, and tracing of inter-channel cross-talk need special attention. A first systematic set of low-level/minimum-bias runs has been taken in fall 2000.

3 Calibration

In November/December 2000, dedicated laser runs were taken to calibrate the detector. The resulting time-offsets (t0's) as well as the exact knowledge of the position of the OMs is a crucial ingredient for the reconstruction of muon tracks. After the data has been taken, the t0's are calculated and, based on the knowledge of the t0's, the position of the OM's was obtained. In February 2001, a preliminary version of the calibration constants were released [8].
A new method, using the numerous atmospheric muons to calibrate the detector, is currently developed and will soon complement the time-consuming laser calibration.

4 Monte Carlo for AMANDA-II

The simulation of AMANDA signal and background can be split into a chain of subprocesses:

- Generation of detectable particles, as atmospheric muons or neutrino induced muons. To generate the atmospheric muon background, we use previously simulated muons from air-showers (`corsika`), which we resampled for a larger detector area. The signal MC consists of an atmospheric ν_μ sample (`nu2mu`), which was already used in the AMANDA-B10 analysis.

- The muons have to be propagated through the surrounding detector medium, by simulating stochastic and continuous energy losses (`mudedx`).

- The detector response is then simulated with the simulation package `amasim`. We thereby provide `amasim` with the configuration of the AMANDA-II detector (geometry, t0's, pulse shapes, noise rates and trigger setting).

Obviously, when moving from AMANDA-B10 to AMANDA-II, the largest changes occur in the detector simulation.
The trigger rate of the experiment (run 296/day 137, dead time corrected), as well as background and signal MC are summarized in table 4.3 [1]. For the observation of atmospheric ν_μ's, the background has to be suppressed by more than 5 orders of magnitude.

experiment	atmospheric μ MC	atmospheric ν_μ MC
75 Hz	53 Hz	$3.5{\cdot}10^{-4}$ Hz

Table 4.3: AMANDA-II trigger rates.

The atmospheric μ MC (assuming an April South Pole atmosphere) predicts $\sim$71 % of the observed rate. Such a discrepancy can barely be explained with theoretical uncertainties. Figure 4.3 shows the frequency of hit multiplicity on trigger level. Hits on OMs with known bad properties have been removed. Besides the previous mentioned difference in normalization, there is a discrepancy at lower hit multiplicities. We believe that both effects are due to a few extremely noisy and cross-talking OMs, which are not simulated and which effectively lower the hit multiplicity trigger. This effect is currently being investigated.

[1] The MC is based on mass00v4 (i.e. the PTD-bug found in 2001 was not yet corrected).

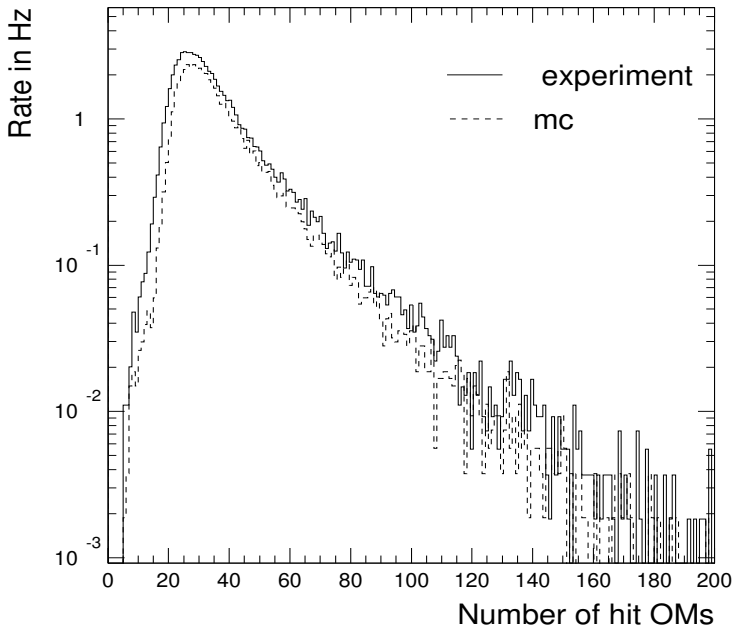

Figure 4.3: Frequency of hit multiplicity for data and atmospheric muon MC.

4.1 Effective Areas after the trigger

Figure 4.4 shows the effective area (at majority trigger level) for different muon energies as a function of the zenith angle. It can be seen that due to the high trigger threshold, the effective area for lower energies is below that of 1997 [2]. The effective area outgrows that of AMANDA-B10 for energies above ∼10 TeV. We note, that the response to lower energy muons is less crucial for a harder energy spectrum, as it is expected from astrophysical sources.

Figure 4.5 illustrates the energy dependent trigger rate for the AMANDA-II detector with a 24- and 13-fold trigger setting as well as for AMANDA-B10 (13-fold majority). Shown are the atmospheric energy spectrum as well as a typical AGN spectrum, with a neutrino flux simulated as $dN/dE = 0.5 \cdot 10^{-6} \cdot (E/GeV)^{-2} \cdot \mathrm{G}eV^{-1}\mathrm{sr\ s^{-1}cm^{-2}}$ (`nusim`). Again, it can be seen that the AMANDA-II configuration with its present 24-fold trigger setting triggers less low energy neutrinos but slightly more high energy neutrinos than the AMANDA-B10 detector. Obviously, AMANDA-II with a 13-fold trigger settings leads to larger neutrino rates at all energies.

Due to a significantly higher signal efficiency on higher cut levels, the observable neutrino rates in AMANDA-II are expected to be higher than in AMANDA-B10. This will be shown in section 6. The gain in sensitivity of AMANDA-II compared to AMANDA-B10

[2] This is expected, since the threshold settings aimed at maximizing the final high energy event sample. Lower energy events are triggered by a "string"-trigger, commissioned in 2001.

will be primarily due to the increase of efficiency $after$ a full neutrino filter.
Figure 4.6 shows the energy spectrum of ν_μ and ν_e events triggered by AMANDA-II ($N_{CH} \geq 24$), both for the atmospheric and for an AGN-like flux. The numbers of charged current events per year amount to 11000 and 162 for ν_μ and 853 and 103 for ν_e, for the atmospheric and the AGN fluxes, respectively [3].

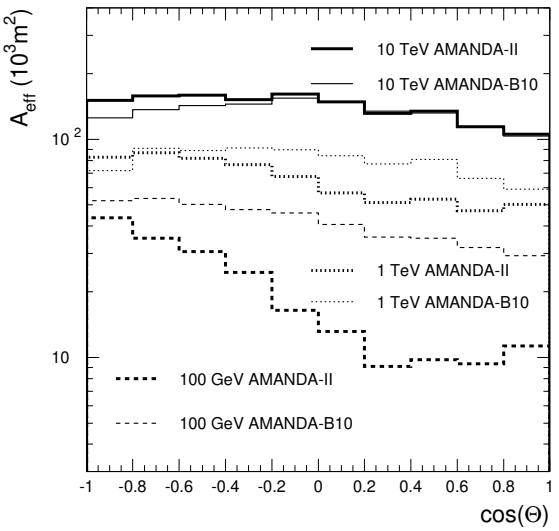

Figure 4.4: Effective area at trigger level for 100 GeV, 1 TeV and 10 TeV muon energies as a function of the zenith angle. The thick line represents AMANDA-II and the thin line AMANDA-B10. Majority trigger are 24 and 13 for AMANDA-II and AMANDA-B10, respectively, which explains the loss in effective area for low energy.

[3] See also the A-II performance paper (R. Wischnewski et al., Proc.27^{th} ICRC, Hamburg,1105(2001)).

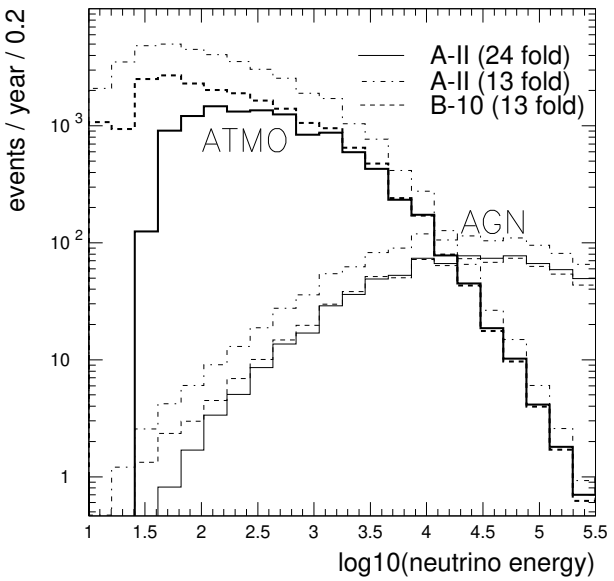

Figure 4.5: Energy distribution of triggering neutrino events for the atmospheric flux and an AGN-like flux with $dN/dE = 0.5 \cdot 10^{-6} \cdot (E/\mathrm{G}eV)^{-2} \cdot \mathrm{G}eV^{-1}\mathrm{sr\ s}^{-1}\mathrm{cm}^{-2}$. Shown are the distributions of the AMANDA-II detector with 13-fold trigger setting (dashed-dotted) and a 24-fold trigger as implemented in 2000 (full line). For comparison we also show the AMANDA-B10 distributions (13-fold, dashed). Neutrino energies are in GeV.

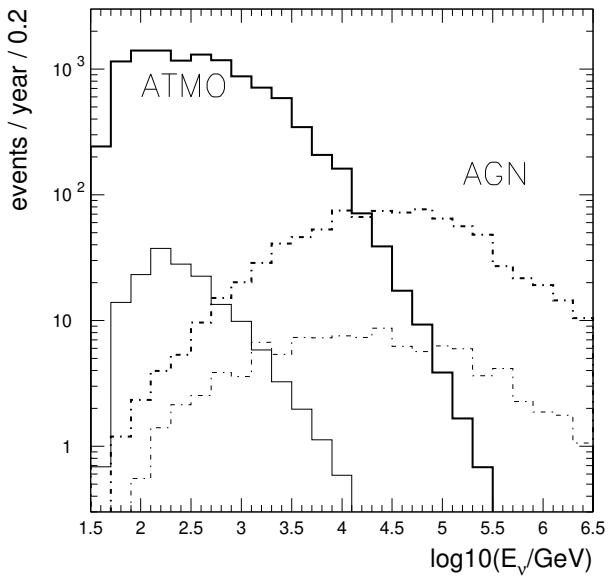

Figure 4.6: Energy distribution of triggering neutrino events with majority trigger 24 in AMANDA-II for the atmospheric flux and an AGN-like flux with $dN/dE = 0.5 \cdot 10^{-6} \cdot (E/\mathrm{G}eV)^{-2} \cdot \mathrm{G}eV^{-1}\mathrm{sr\ s}^{-1}\mathrm{cm}^{-2}$, for ν_μ and ν_e events (upper and lower curves, respectively).

5 The B10 sub-detector in comparison with 1997

As a first check of the detector performance we compared AMANDA-II data, reduced to the B10 part, with AMANDA-B10 data taken in 1997. Malfunction of the detector in 2000 would appear in direct observables as e.g. number of hit OMs or hit frequency per channel or would show up after track reconstruction. We compared run 540/day 109 from 1997 to run 296/day 137 from 2000.
To obtain the same conditions for both data sets the following preprocessing was applied:

- common trigger condition: In 1997 the multiplicity trigger was set to 16 hits within a time window of 2μs. In 2000, the threshold was 24 coincident hits in all 19 strings within 2.5μs. For the comparison we only consider events with $\geq$24 hits in strings 1-10 during 2μs.

- All "bad" OMs which were excluded in 1997 *or* are rejected in the present 2000 analysis are excluded for this comparison. These are 42 rejected OMs out of 302 in total (34 were classified as bad in 1997, 36 in 2000).

The dead time corrected event rates after preprocessing, R^{24}, and after level 1 cuts , R^{L2}, as well as the dead time are listed in table 5.4. The agreement in event rates indicates a similar behaviour of the B10 sub-detector at trigger level for both data sets. We note, that for a precision rate comparison the seasonal muon rate variation needs to be accounted for (see fig.2.2 and [6]). They would suggest an up to $\sim$5% (or $\sim$1.3 Hz) higher event rate for the 1997 data set due to the 28 days seasonal difference between both selected runs. Fig 5.7 b) indicates a decrease in the rate of hit OMs in strings 1-4 by $\approx 10\%$ which leads to a slight shift in the total number of hit OMs per event (fig. 5.7a). This discrepancy as well as the higher rate at large channel multiplicities has to be further investigated.

	1997	2000
R^{24} [Hz]	25.9	26.0
R^{L2} [Hz]	0.035	0.038
t_{dead} [%]	24.0	17.6

Table 5.4: Dead time corrected event rates after preprocessing (R^{24}) and after level 1 cuts (R^{L2}), dead time fraction in 1997 and 2000.

We applied the standard level 1 and 2 reconstruction from the 1997 analysis to this data sample. The level 1 results for angular distributions of the "line fit" and the "pandel fit" (see sect. 6) are shown in fig. 5.8. There is good agreement for both the 1997 and 2000 data sets over the whole zenith angle range.
After applying level 1 cuts ($\theta_{LF} > 70^o$, $v_{LF} > 0.1\,\mathrm{m/ns}$, $\theta_{pandel} > 70^o$) we performed a second level reconstruction as in the 1997-DESY analysis [3]. The zenith angle distribution of the iterative maximum likelihood reconstruction (fig. 5.9) agrees well in the range of

events reconstructed as downgoing. Only at zenith angles $\theta \geq 90^o$ a small excess in the 2000 data is seen.
To summarize, we find for the B10 part of AMANDA-II compared to 1997 B-10 data reasonable agreement from trigger level down to cut-level 2.

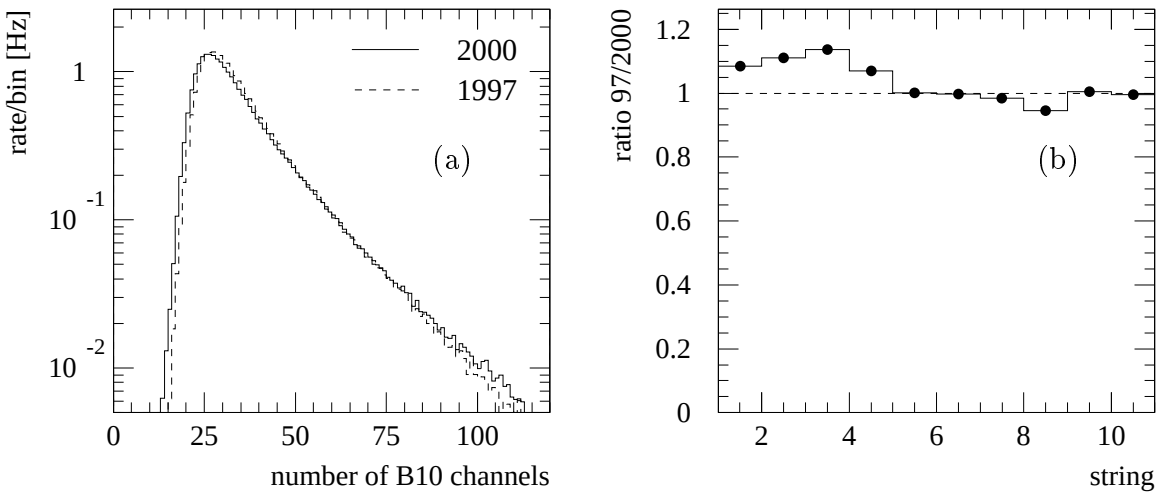

Figure 5.7: a) Number of hit OMs in the B10 sub-detector after cleaning in 1997 and 2000;
b) Ratio (1997:2000) of hit frequency, averaged over single strings.

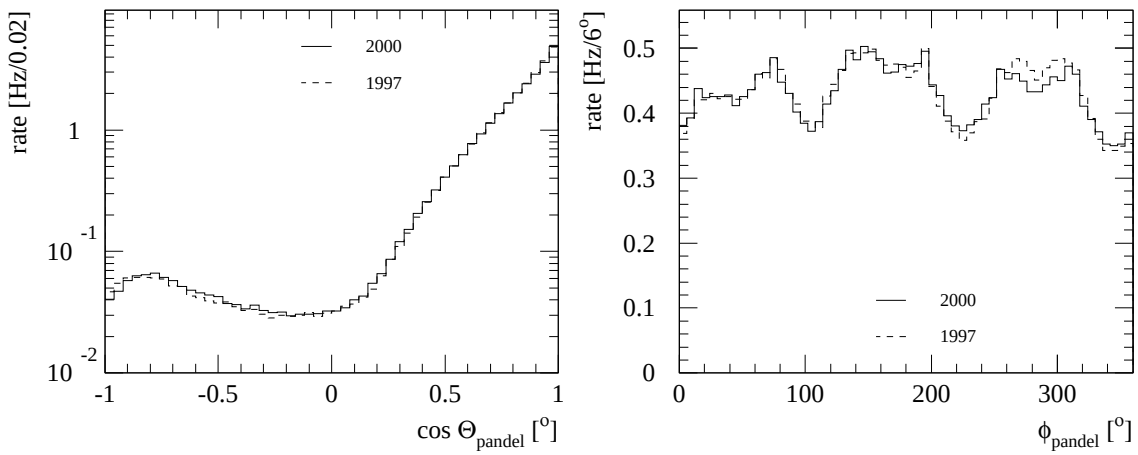

Figure 5.8: Results of the pandel fit at level 1: The solid (dashed) line shows the distributions of zenith and azimuth angle from 2000 (1997) data.

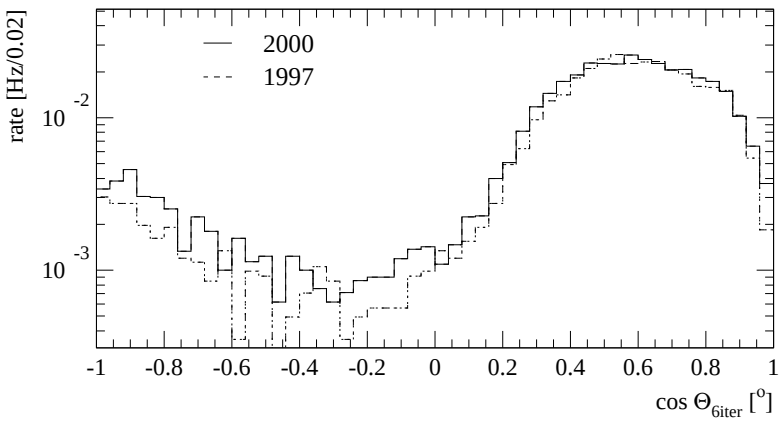

Figure 5.9: Zenith angle distribution after level 1 cuts (iterated pandel fit).

6 First steps in the analysis

This analysis investigates the performance of first and second level filters for AMANDA-II. Additionally, we give an outlook on the capability of AMANDA-II to separate atmospheric ν_μ's from the background of atmospheric μ's. We use the reconstruction tools which were developed for the AMANDA-B10 analysis. We apply a new combination of cuts, tailored for AMANDA-II. We believe that, due to the increase of detector-size, it is possible to obtain a simpler and more efficient filter. We are confident that we can reach the atmospheric neutrino level with a larger signal efficiency than in the analysis of the 1997 data. As for 1997, we divide the analysis into separate levels, which are described below. The data which we have investigated, consists of 14 hours of experimental livetime (run 304/day 145), 5.4 hours of atmospheric μ MC (background) and 55 days of atmospheric ν_μ MC (signal).

6.1 Level-1 and level-2

The first levels aim at reducing the data sample to a size small enough to allow more time consuming likelihood reconstructions. Level-1 and level-2 are summarized in table 6.5. Level-1 consists of a fast analytic reconstruction ("line fit") and a cut on the reconstructed zenith angle. Appended is a likelihood reconstruction ("pandel fit"). Level-2 includes 3 more cuts as well as more sophisticated reconstructions [3], as for example a 16-iteration likelihood reconstruction.

The filter efficiency of level-1 and level-2 for the experiment, background and signal MC are summarized in table 6.6. After level-2, there are $\sim 2 \cdot 10^4$ events/day left, containing on average $\sim$23 atmospheric neutrinos. We note that the signal efficiency at this stage is considerably higher than in the previous AMANDA-B10 analysis. For a comparable background suppression, the efficiency for the signal is about 2-3 times larger than in the AMANDA-B10 analysis.

The left of figure 6.10 shows the distributions of the reconstructed zenith angle of the background for trigger level (level-0), after level-1 and after level-2. On level-0 and level-1, the MC distribution agrees roughly with that of the experiment. For level-2, a disagreement can be observed in the tails of the distribution ($\cos\theta < 0$). The right plot shows the distribution of the true zenith angle of the atmospheric ν_μ MC. It can be seen that after level-2, the signal is reduced only little, even close to the horizon. Compared to the AMANDA-B10 analysis, where the signal efficency at the horizon decreases significantly, this is an improvement.

Summarizing we can say, that with fewer cuts, while still preserving the largest part of the signal, a significant background rejection is possible.

Id	Name	Remarks
Level-1		
Reco 1	Line-fit	
Cut 1	$\theta(1) > 70^\circ$ [$\theta(1) < 90^\circ$]	Zenith Line-fit
Reco 2	U-Pandel likelihood	Single photon arrival time probabilities
Reco 3	Dipole approximation	
Reco 4	Tensor of Inertia	
Level-2		
Cut 2	$\theta(2) > 80^\circ$	Zenith, Reco 2
Cut 3	$N_{direct}^{-25..75}(2) > 3$	Number of direct hits, Reco 2
Reco 5	Iterative U-Pandel	16 iterations
Cut 4	$\theta(3) > 80^\circ$	Zenith, Reco 3
Reco 6	Energy reconstruction	$P_{hit} * P_{nohit}$, using Reco 5

Table 6.5: Overview of the reconstructions and cuts from level 1 and level 2.

	exp data	atmospheric μ MC	atmospheric ν_μ MC
Level-0	$3.7 \cdot 10^6$ (events/14 hours)	$1.0{\cdot}10^6$ (events/5.4 hours)	1677 (events/55 days)
Level-0	1.0	1.0	1.0
Level-1	$7.5 \cdot 10^{-2}$	$7.0 \cdot 10^{-2}$	0.89
Level-2	$3.3 \cdot 10^{-3}$	$2.4 \cdot 10^{-3}$	0.75

Table 6.6: Compilation of experimental and Monte Carlo statistics and filter efficiencies. The first row shows the statistics of the experimental data, the background and the signal MC. The rows 3 and 4 show the fraction of triggering (level-0) events which pass the level-1 and level-2 cuts.

6.2 Beyond level-2

To give a rough estimate of the capability of AMANDA-II as a neutrino-detector, we present a set of very preliminary neutrino-cuts. The cut variables used are the final cut variables from level-4 of the Zeuthen 1997 neutrino analysis [3]:

- $|S^{van}|$: The ("vanilla") smoothness measures the homogeneity of the distribution of hits along the track. This cut is motivated by the fact that Cherenkov light is emitted continuously.

- $|S^{phit}|/(\theta - 75^\circ)$: This cut parameter compares the reconstructed zenith angle to the "phit" smoothness (the above mentioned smoothness, where every hit is weighted with its hit probability). This variable is slightly modified, to account for the better reconstruction abilities of AMANDA-II.

- $(N_{dir}(-15:75) - 2) \cdot L_{dir}(-15:75)$: The number N_{dir} of OMs hit by "direct" ("unscattered") photons (reduced by 2), multiplied with the largest distance between

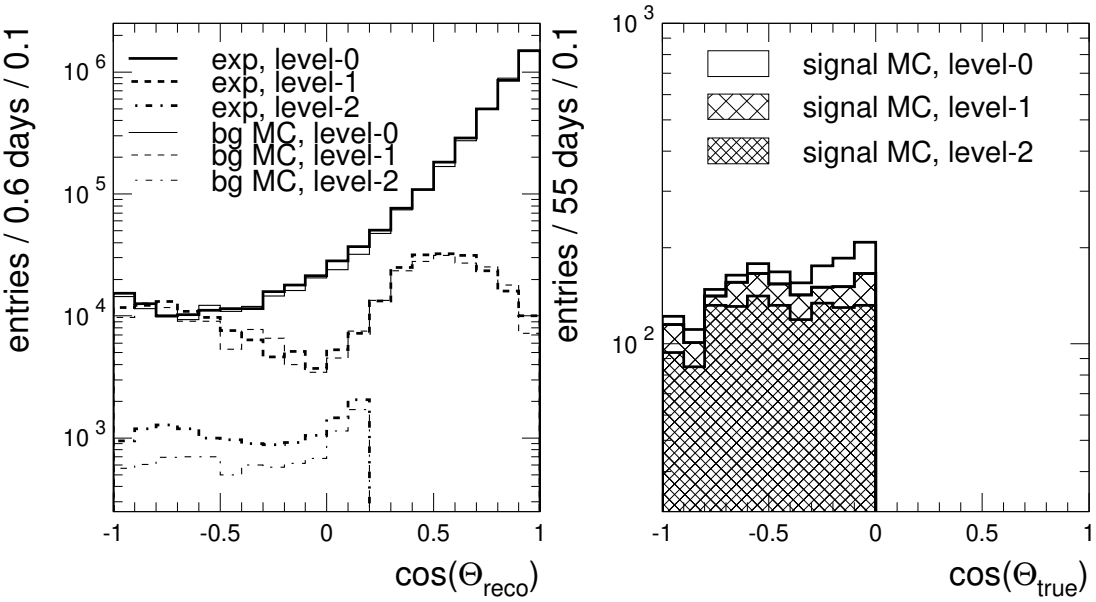

Figure 6.10: Left: Distribution of the reconstructed zenith angle, θ_{reco}, for the experiment (thick line) and atmospheric μ background MC (bg, thin line) at trigger level (level-0, full line), level-1 (dashed line) and level-2 (dash-dotted line). The reconstructions used are the best available on the corresponding level (Reco 1, Reco 2, Reco 5 from table 6.5). All curves are normalized to the experiment on level-0.
Right: Distribution of true zenith angle, θ_{true}, of atmospheric ν_μ MC (`nu2mu`) for the different levels. The neutrinos were only generated with $\cos\theta < 0$.

any two of these OMs. We interpret this observable as the lever-arm of the fit times the number of strong supporting points in between. Here, the definition of direct photons is such that they arrive at most 15 ns too early or 75 ns too late as compared to the expectation for truely un-scattered photons.

- $\log(\mathcal{L}_{up}/\mathcal{L}_{down})$: The ratio of likelihoods of the reconstruction between the best upward moving and the best downward moving track hypothesis.

- $\Psi(16iter, LF)$: The space angle between the 16 iteration likelihood reconstruction and the line fit.

- $COGz$: The z-coordinate of the "center of gravity" of the position coordinates of all hit OMs. This cut is not included within level-4, but within level-3 of the 1997 Zeuthen analysis.

- $\theta_{reco} > 95°$: The final cut is a cut on the reconstructed zenith angle of the 16 iteration likelihood reconstruction.

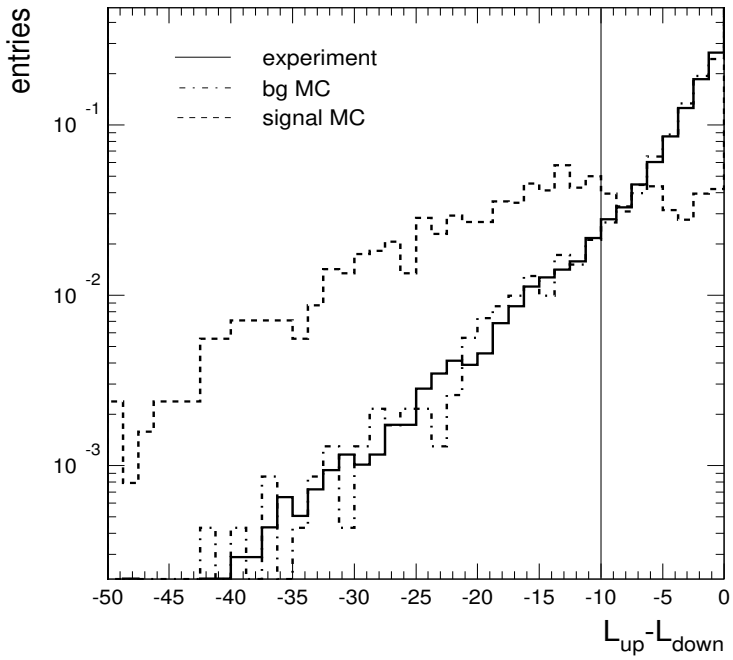

Figure 6.11: Normalized distributions of the cut variable, $\mathcal{L}_{up} - \mathcal{L}_{down}$, for the experiment, atmospheric μ MC and atmospheric ν_μ MC, after level-2 cuts. The cut value is indicated by the straight line.

The cut values were adjusted "by hand", as to reduce the number of experimental events, to the order of expected atmospheric ν_μ events. As an example, we show the distribution of $\mathcal{L}_{up} - \mathcal{L}_{down}$, after level-2 cuts in figure 6.11.

After application of the cuts, 6 events are left. Expected are on average 3.9 atmospheric ν_μ events. This corresponds to an atmospheric ν_μ efficiency of 22 %. Figure 6.12 shows the distribution of the reconstructed zenith angle of the final events, as well as that expected from atmospheric ν_μ's.

At this stage, with not enough background MC statistics (5.4 hours, 0 events passing the cuts) available, it is difficult to proof that the remaining 6 events contain neutrinos. However, by visual inspection, we find at least 3 rather promising candidates. The event with an incident angle closest to the horizon is shown in the appendix A. It has a reconstructed zenith angle of 106° and a neutrino-like appearance. Such horizontal events are predicted by the signal MC. The ability to reconstruct events close to the horizon should be viewed as one of the fundamental benefits of the additional outer strings of AMANDA-II.

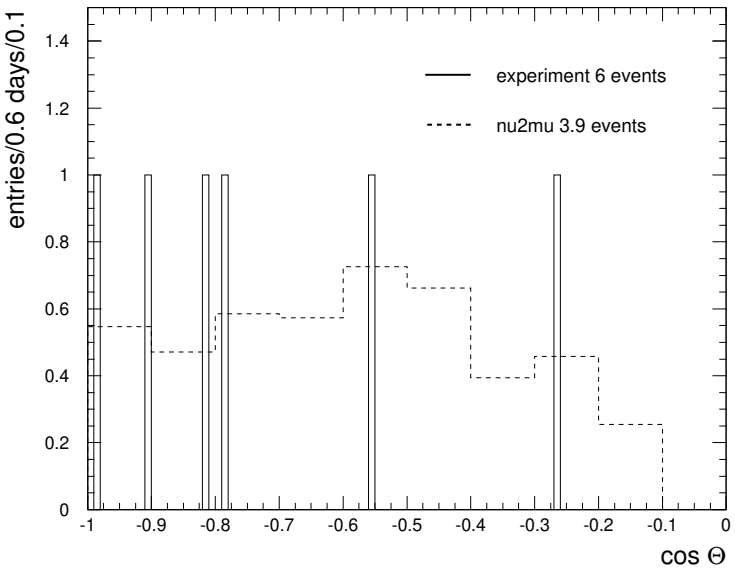

Figure 6.12: Distribution of the reconstructed zenith angle of the events passing the beyond-level-2 cuts.

7 Conclusions

We have presented a brief summary of the analysis of the data taken in 2000 with the AMANDA-II detector. We presented an investigation of detector performance over the year, the adjustment of the detector Monte Carlo to the enlarged detector, and the development of an analysis chain and selection criteria for atmospheric neutrinos. We have demonstrated the functionality of the 10 string sub-detector, by comparing its performance with the AMANDA-B10 detector operated in 1997.

To illustrate the capabilities of AMANDA-II, we applied a preliminary filter (beyond level-2) to 14 hours of detector livetime. We observe 6 events, of which at least 3 have a neutrino-like appearance (from visual inspection). The atmospheric ν_μ MC predicts 3.9 events. Of the presently available 5.4 hours of atmospheric μ MC, no event passes. The combined analysis of the AMANDA-B10 data resulted in about 2 events per day lifetime [3, 4], while from our cuts we derive a (very preliminary) value of 6.7 events per day for the atmospheric ν_μ MC. We emphasize, that for harder energy spectra from astrophysical neutrino sources, an even larger improvement from AMANDA-B10 to AMANDA-II is expected. For the analysis presented here, the filter efficiencies for atmospheric ν_μ MC (22%) is roughly 4 times larger than in the AMANDA B-10 neutrino analysis. The AMANDA-II sensitivity is found to be high even close to the horizon.

The generation of a larger sample of background MC is underway. This will enable us to properly investigate, as well as optimize, our filter beyond level-2. In parallel, processing of experimental data is continued.

A The neutrino candidate closest to the horizon

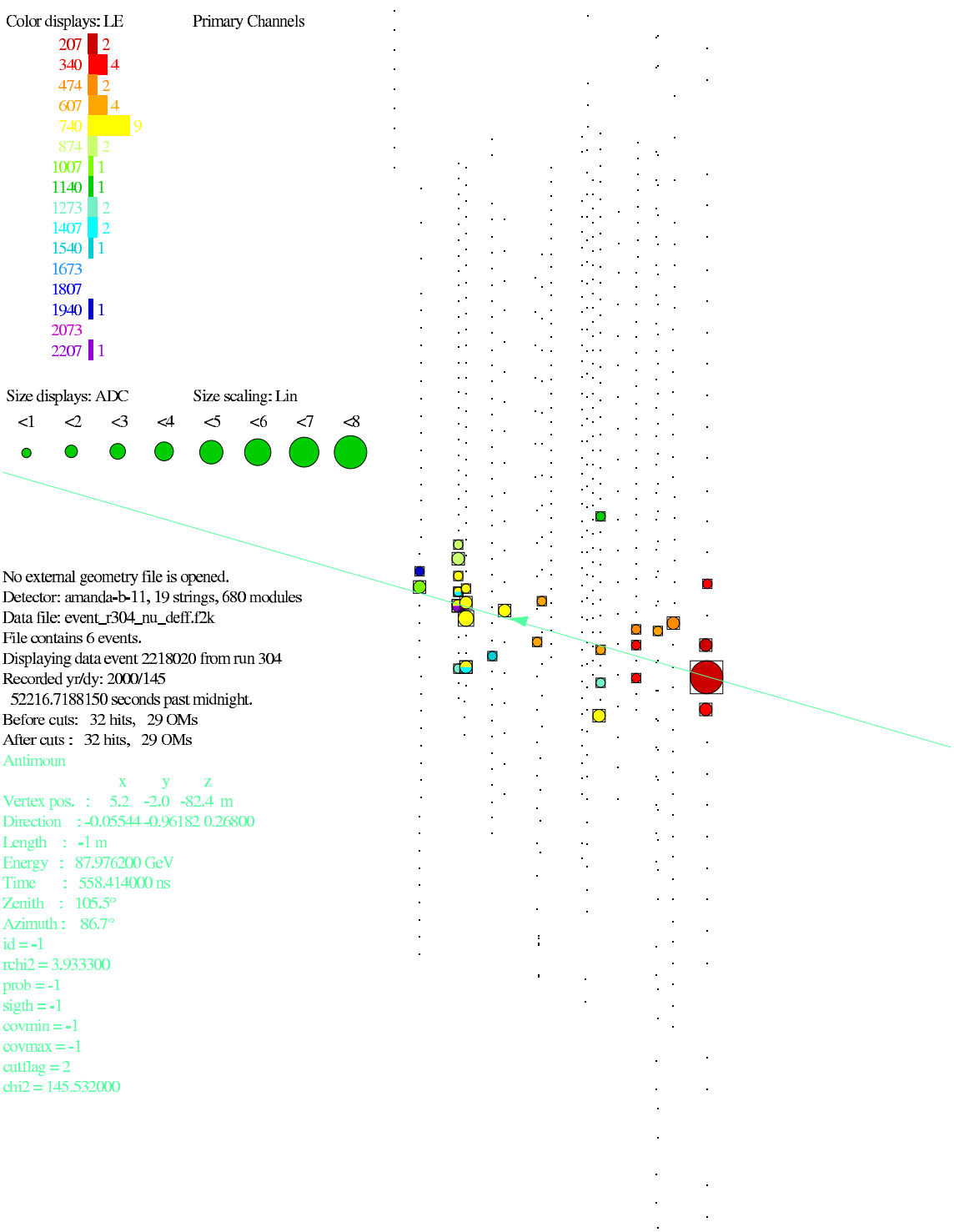

References

[1] E. Andres *et al.* [AMANDA Collaboration], Astropart. Phys. **13** (2000) 1.

[2] E. Andres *et al.*, Nature **410** (2001) 441.

[3] A. Biron *et al.* [DESY-Zeuthen], Detection of Atmospheric Neutrinos in 97 Data, AMANDA-Internal report, April 2001.

[4] T. DeYoung *et al.*, Talk at AMANDA-Meeting, LagunaBeach, Sept.2000, and PhD-Thesis, in preparation.

[5] J. Ahrens *et al.* [AMANDA Collaboration], Search for Supernova Neutrino-Bursts with the AMANDA Detector, submitted to Astropart. Phys.

[6] A. Bouchta *et al.* [AMANDA Collaboration], Seasonal variation of the muon flux seen by AMANDA, Proceed. of XXth ICRC, Salt Lake City, 1999.

[7] A. Biron *et al.*, First and Second Level Reconstruction of 1997 Muon Data, AMANDA Internal Report 19990701.

[8] K. Woschnagg *et al.*, AMANDA Collaboration meeting, Bartol, March 2001.